TIRE LUG HEIGHT EFFECT ON SOIL STRESSES AND BULK DENSITY

T. R. Way, A. C. Bailey, R. L. Raper, E. C. Burt

ABSTRACT. *Soil stresses and increases in soil bulk density were measured beneath the centerline of one new 18.4R38 radial-ply R-1 tractor tire and two similar tires with lug heights of 55% and 31% of the new tire lug height. Each tire was operated with an inflation pressure of 110 kPa, a dynamic load of 25.0 kN and 10% slip. Soil stress state transducers (SSTs) measured the stresses at three depths in both a hardpan soil profile and a uniform soil profile, each in a sandy loam and a clay loam soil. The initial depths of the SSTs ranged from 164 to 288 mm. Analysis of the original soil stress data showed that lug height did not significantly affect the peak octahedral normal stress or its corresponding octahedral shear stress. When outliers were removed from the peak stress data, however, lug height significantly affected the octahedral normal stress in the sandy loam soil. In the uniform profile of the sandy loam and in the hardpan profile of the clay loam, the new tire generated the greatest bulk density increase, which was significantly greater than the bulk density increase caused by the 55% tire. In the sandy loam with the hardpan profile, the 55% lug height tire generated a significantly greater bulk density increase than either the new or 31% tire.* **Keywords.** *Soil compaction, Soil dynamics, Tires, Traction, Sensors.*

Soil compaction in the crop root zone has the potential to inhibit plant growth and reduce crop yields. Compaction caused by tractor tires has been shown to reduce water infiltration rates (Vomocil et al., 1958), which may cause increased runoff and decreased availability of water to plants.

The lug height of a tire operating on soil is likely to affect soil compaction near the soil surface more than at deeper depths. As the lug height increases, compaction of the soil beneath the imprints of lugs is expected to increase and that beneath the imprints of the undertread is likely to decrease. Infiltration of water into the soil is expected to decrease as lug height increases because water tends to accumulate in the lug imprints, where compaction is greatest.

Most of the research of tractor tire lug heights has reported the effect of lug height on tractive performance. The effect of lug height on soil stresses and soil compaction has seldom been mentioned. The stress state in soil beneath an 18.4-38 pneumatic tire with no lugs was measured by Bailey et al. (1988). The major principal stress, mean normal stress and octahedral shearing stress generally were greater for transducers whose initial depth was 300 mm than those with an initial depth of 450 mm. Comparisons were not made with stress states generated by a tire with lugs.

Article was submitted for publication in June 1994; reviewed and approved for publication by the Power and Machinery Div. of ASAE in February 1995. Presented as ASAE Paper No. 93-1033.

Mention of trademarks or company names does not imply endorsement of these products by the USDA.

The authors are **Thomas R. Way,** ***ASAE Member Engineer,*** Agricultural Engineer, **Alvin C. Bailey,** ***ASAE Member Engineer,*** Agricultural Engineer, and **Randy L. Raper,** ***ASAE Member Engineer,*** Agricultural Engineer, and **Eddie C. Burt,** ***ASAE Member Engineer,*** Research Leader, USDA-Agricultural Research Service, National Soil Dynamics Laboratory, Auburn, Ala.

Tractive performances of new and worn 18.4R38 radial-ply R-1 tires on the rear axle of a MFWD tractor operating on a disked sandy clay soil were determined by O'Brien (1991). Slip resulting from a given drawbar pull generally increased as lug height increased.

Tractive performances of five 13.6-38 tractor drive tires with lug heights of 0, 20, 35, 50, and 75 mm were measured on clay, clay loam, sandy loam, and sandy clay loam soils, with disked, plowed, cultivated, and various vegetative and residue surfaces (Gee-Clough et al., 1977). Lug heights greater than 20 mm did not improve performance in poor tractive conditions and they decreased performance in average tractive conditions.

Tractive performances of 11-38 tires with lug heights from 13 to 44 mm were measured by Reed and Shields (1950). Tractive efficiency decreased as lug height increased on a loose Norfolk sandy loam, a Hiwassee sandy loam and a Decatur clay loam soil.

Observations of tire operation have shown that, under some lug height and soil conditions, only the lug face of the tire contacts the soil. Conversely, in freshly tilled soil conditions, the entire tread surface, both lug face and undertread, are in contact with the soil. These apparent differences in soil-tire interaction caused us to suspect that lug height may affect soil compaction. Therefore, an experiment was developed with the following objectives:

- Determine the effect of lug height of radial-ply R-1 tires on the soil stress state and soil compaction.
- Determine the effect of depth beneath the soil surface and the effect of soil profile on soil stresses and compaction.

MATERIALS AND METHODS

The experiment was conducted at the National Soil Dynamics Laboratory (NSDL), a facility of the USDA-Agricultural Research Service in Auburn, Alabama, using

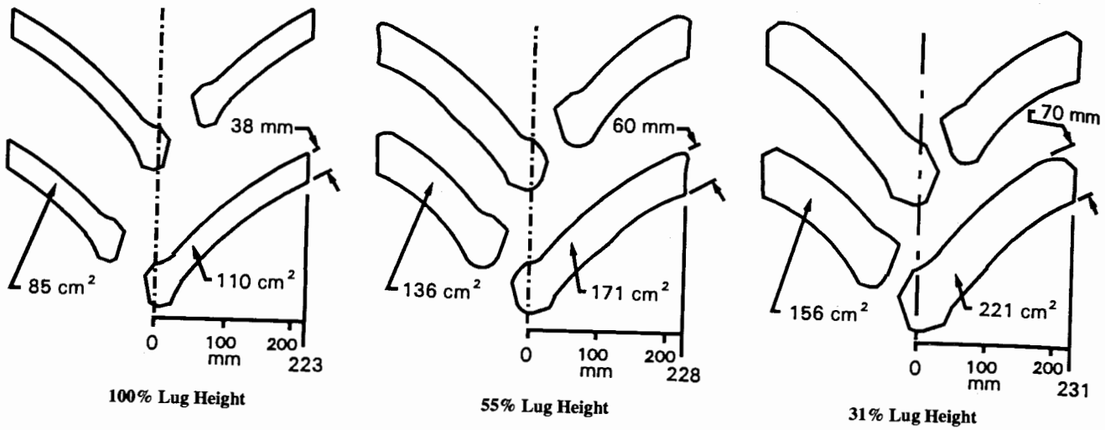

Figure 1–Lug patterns, lug widths, and lug face areas of the tires.

the NSDL single wheel traction research vehicle described by Burt et al. (1980). Three 18.4R38 Armstrong Hi-Traction Lug Radial (1-Star) R-1 tires were powered by the traction research vehicle, one at a time. Each tire had 30 long and 30 short lugs with the lug patterns shown in figure 1. One tire was new, with full lug height, and its lug height was designated as 100%. The lugs of the other tires were hand-buffed so the mean lug heights of the long lugs at the circumferential centerline were 31% and 55% of the corresponding mean lug height of the new tire (fig. 2). The mean lug heights of the long lugs at the circumferential centerlines of the tires were 43.3, 23.7, and 13.4 mm for the 100, 55, and 31% tires, respectively. Lug taper (ASAE, 1993) caused the area of the lug faces to increase as lug height decreased.

The experiment was conducted on NSDLs two indoor soil bins, one containing Norfolk sandy loam soil (NSL) (Typic Paleudults) and the other containing Decatur clay loam soil (DCL) (Rhodic Paleudults). The content of the NSL was 71.6% sand, 17.4% silt, and 11.0% clay, and the content of the DCL was 26.9% sand, 43.4% silt, and 29.7% clay. Each soil bin was prepared twice to obtain two different density profiles. The 'hardpan profile' was established in each soil by first rotary tilling the soil to a depth of about 600 mm. A hardpan was formed across the whole area of each bin by using a single moldboard plow followed by a steel wheel operating in the plow furrow. The loose soil above the hardpan was leveled with a scraper blade after the hardpan was formed. The top of the hardpan was 288 mm beneath the loose surface of the NSL soil and 324 mm beneath the loose surface of the DCL soil. The second profile of each soil was the "uniform profile" and was formed by rotary tilling to a depth of about 600 mm and then leveling the surface of the soil with a scraper blade. Initial conditions of the soils are given in table 1.

For each combination of soil and profile, the lug height treatments were assigned to the plots in a randomized block pattern. Each soil bin was divided into four blocks (replications), each containing three plots, one for each lug height.

Three stress state transducers (SSTs) were used to measure stresses in the soil beneath the tires. Each SST consisted of pressure sensors with diaphragm diameters of 9.7 mm, mounted on a machined aluminum block, and otherwise was similar to the modified SST described by Nichols et al. (1987) (fig. 3). Each SST measured six soil pressures which were used to calculate the complete stress state of the soil at the transducer. The stress state may be represented by stresses on particular planes, such as the octahedral shearing (τ_{oct}) and normal (σ_{oct}) stresses and their directions. The octahedral normal stress is also called the mean normal stress. The octahedral stresses are described by Grisso et al. (1987).

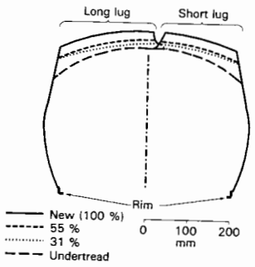

Figure 2–Circumferential projections of lugs and undertread of unloaded tire sections onto a cross-sectional plane when inflation pressures were 110 kPa.

Table 1. Mean initial conditions of soils

Soil	Profile	Moisture Content Above Hardpan Depth (% d.b.)	Bulk Density: In Loose Soil* (Mg/m^3)	Bulk Density: In Hardpan (Mg/m^3)	Soil Cone Index† (kPa): Depth Beneath Untrafficked Surface (mm) 0-50	0-288	288-348
NSL	Uniform	6.6	1.235	—	244	567	1060
NSL	Hardpan	6.9	1.159	1.745	217	591	7420
					Depth Beneath Untrafficked Surface (mm) 0-50	0-324	324-384
DCL	Uniform	12.7	1.171	—	245	872	1970
DCL	Hardpan	13.6	1.185	1.602	286	1040	5080

* Depth of center of loose soil sample beneath untrafficked soil surface was 144 mm in the NSL and 162 mm in the DCL.

† Base area of cone penetrometer = 323 mm^2. Each cone index is the mean of 12 cone penetrations.

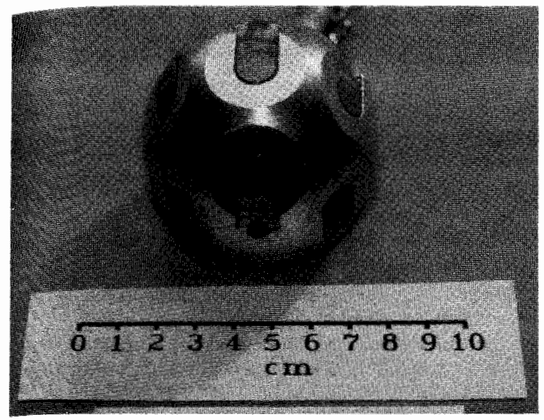

Figure 3–Stress state transducer (SST).

The three SSTs were buried in the soil beneath the centerline of the tire path to be trafficked, and the tire was then operated on the soil. The center of the pressure measurement for each SST was assumed to be the mean vertical position of the top and lower pressure sensor diaphragms, which was 14 mm beneath the top of the SST. In each plot, each SST was buried at one of the three depths for that soil as shown in table 2. In the hardpan profile of each soil, the deep SSTs rested on the hardpan and the same initial depth was used for the deep SSTs in the uniform profile.

For all tests, the forward velocity was 0.15 m/s, slip was 10%, the tire inflation pressure was 110 kPa, and the dynamic load was 25.0 kN, which is the recommended load for the 110 kPa inflation pressure. All variables were controlled by computer throughout each test. The data acquisition system read each transducer once per 25 mm of distance traveled. Zero conditions for slip calculations consisted of zero net traction with each tire operating on concrete. The computer program that controls the traction research vehicle was designed to align a chosen point on the tire tread directly above a particular SST when the point was at the bottom dead center position. In this experiment, the end of a long lug at the circumferential centerline of the tire was chosen for alignment above the first in each series of three SSTs. Because the three tires had different rolling radii, the longitudinal position of a long lug relative to each SST was not constant. The theoretical maximum longitudinal misalignment of the end of a long lug relative to each SST was 26 mm. The inability of the traction research vehicle to accurately control the longitudinal alignment caused some deviation from the 26 mm theoretical maximum.

Soil samples were collected after the tests were completed to determine soil moisture content and bulk density. In each plot, three soil samples were taken beneath the tire track to determine bulk densities. Each sample was taken beneath the imprint of the end of a long lug at the centerline of the tire track, one sample at the same final depth of each SST. A fourth sample was taken in the untrafficked soil in each plot. In the hardpan profile, the fourth sample was taken above the hardpan and a fifth sample was taken in the compacted soil in the hardpan beneath untrafficked soil. The bulk density increase was calculated using equation 1:

$$bd_{inc} = [\,(bd_f - bd_i) / bd_i\,] \times 100\% \qquad (1)$$

where

bd_{inc} = bulk density increase (%)
bd_f = final dry bulk density beneath tire track (Mg/m^3)
bd_i = initial dry bulk density (untrafficked soil) (Mg/m^3)

Table 2. Mean depths of SST centers of pressure measurement beneath untrafficked soil surface

Depth Designation	NSL: Initial (Both Profiles) (mm)	NSL: Final, Uniform Profile (mm)	NSL: Final, Hardpan Profile (mm)	DCL: Initial (Both Profiles) (mm)	DCL: Final, Uniform Profile (mm)	DCL: Final, Hardpan Profile (mm)
Shallow	164	280	202	164	259	205
Intermediate	209	305	228	209	291	235
Deep	252	335	257	288	341	294

Results and Discussion

The original data were transformed by subtracting the longitudinal position of the axle from the longitudinal position of the SST to represent pressures and stresses in the soil relative to the axle. An example of pressure data sensed by the six individual pressure sensors of an SST is shown in figure 4. The value of 0 on the distance axis represents the longitudinal position of the wheel axle. Data at positive distance values represent pressures in front of the axle and data at negative distances represent pressures to the rear of the axle. The pressures applied to the sensors on each SST were designated p_x, p_y, p_z, p_1, p_2, and p_3. Each SST was buried with the p_x diaphragm normal to the longitudinal direction, facing opposite the direction of travel, the p_y diaphragm normal to the lateral direction, facing to the right of the tire and the p_z diaphragm facing

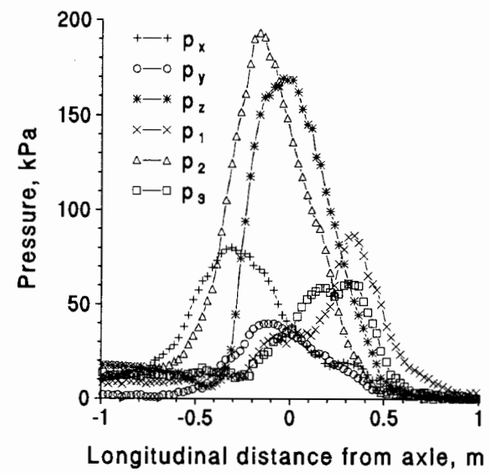

Figure 4–Pressures measured by an SST in the NSL with the hardpan profile, buried at the deep depth beneath the centerline of the 55% lug height tire.

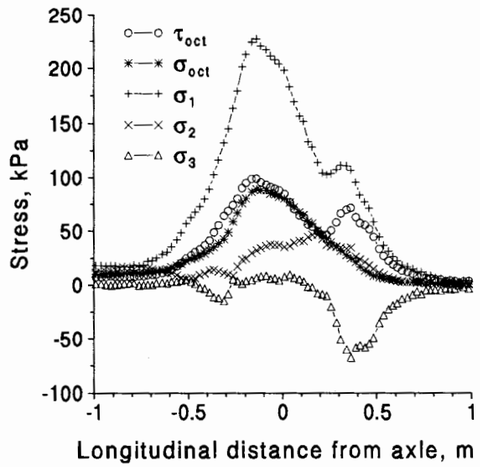

Figure 5–Calculated stresses from data shown in figure 4.

up. Normals to the p_1, p_2, and p_3 diaphragms were each tilted 54.7° downward from vertical. The p_1 diaphragm faced the upward right rear direction, the p_2 diaphragm faced the upward right front direction and the p_3 diaphragm faced the upward left rear direction.

The SST data typically showed that the peak pressure on the p_2 diaphragm exceeded the peak pressure on the p_z diaphragm (fig. 4). Apparently the peak pressure applied to the p_2 diaphragm is comprised of a component in the longitudinal direction caused by the net traction of the tire, in addition to a component in the vertical direction resulting from dynamic load, and the resultant was therefore greater than the peak pressure on the p_z diaphragm.

The calculated principal stresses (σ_1, σ_2, and σ_3) and the octahedral stresses (σ_{oct} and τ_{oct}) for the data in figure 4 are shown in figure 5 using the same distance axis. Further analyses were conducted using two stresses from each SST in each plot: the peak octahedral normal stress, σ_{oct}, and the octahedral shear stress, τ_{oct}, that occurred at the same longitudinal position relative to the wheel axle. Mean values of σ_{oct} and τ_{oct} for the four replications of the lug height treatments, SST depths, soils, and profiles are shown in table 3.

A separate analysis of variance was done for each soil because the initial depth of the deep SST differed for the two soils. Replication was nested within profile. SAS programs were used to evaluate the effect of the independent variables lug height, SST depth and profile, and their interactions on the dependent variables σ_{oct} and τ_{oct}, and the soil bulk density increase (SAS Institute, Inc., Cary, N.C.).

In five of the 72 SST data sets, pressures that were greater than usual were measured by an individual pressure sensor on an SST. The method of outlier detection described by Murphy (1950) detected three values of σ_{oct} and five values of τ_{oct} as outliers. A second statistical analysis using SAS was performed with these 8 of the total of 288 values treated as missing values. The only difference between the original statistical analysis and the missing value analysis was the use of missing values in SAS to replace the outliers in the second analysis. The coefficients of variation for the missing value analysis decreased considerably relative to the original analysis (table 4). A discussion of both analyses follows.

Table 4. Coefficients of variation for original and missing value analyses of octahedral stresses

	NSL		DCL	
Dependent Variable	Original Analysis (%)	Missing Value Analysis (%)	Original Analysis (%)	Missing Value Analysis (%)
σ_{oct}	33.5	14.0	42.3	32.5
τ_{oct}	58.8	24.2	61.2	40.9

Analysis of Original Octahedral Stress Data

Profile was the only variable that significantly affected σ_{oct} and τ_{oct} in the NSL. The analysis of variance showed that profile significantly affected σ_{oct} ($p = 0.0001$) and τ_{oct} ($p = 0.0007$) (table 5). In the NSL, lug height did not significantly affect either σ_{oct} ($p = 0.6309$) or τ_{oct} ($p = 0.3934$) and the SST depth did not significantly affect either σ_{oct} ($p = 0.8731$) or τ_{oct} ($p = 0.2730$). MANOVA, which is the multivariate option of SAS, was used to analyze both octahedral stresses jointly. The MANOVA analysis for the NSL found profile to significantly affect σ_{oct} and τ_{oct} jointly ($p = 0.0128$). The significantly greater octahedral stresses in the hardpan profile exhibit an expected trend because stresses above a hardpan, particularly at a depth near the hardpan, are expected to be greater than those at the same depth in a uniform profile.

None of the independent variables or interactions significantly affected the octahedral stresses in the DCL soil at the 5% level of significance. Lug height did not significantly affect either σ_{oct} ($p = 0.9977$) or τ_{oct} ($p = 0.6573$), profile did not affect either σ_{oct} ($p = 0.3563$) or τ_{oct} ($p = 0.5132$), and the SST depth did not affect either σ_{oct} ($p = 0.1693$) or τ_{oct} ($p = 0.2100$).

Table 5. Effect of soil profile on σ_{oct} and τ_{oct} in the NSL soil for the original statistical analysis

Profile	σ_{oct} (kPa)	τ_{oct} (kPa)
Uniform	76a*	86a
Hardpan	115b	149b

* Within columns, means followed by the same letter are not significantly different (alpha = 0.0007).

Analysis of Octahedral Stress Data with Missing Values

In the missing value analysis for the NSL, σ_{oct} was affected by both lug height ($p = 0.0198$) and profile ($p = 0.0001$), and τ_{oct} was significantly affected by profile ($p = 0.0001$). The trend of decreasing σ_{oct} with decreasing lug height in the NSL soil was an expected result (table 6). Significant effects of profile on the octahedral stresses for the missing value analysis (table 7) were the same as those for the original analysis (table 4). The results of MANOVA showed that profile significantly affected σ_{oct} and τ_{oct} jointly ($p = 0.0041$).

The missing value analysis for the DCL found none of the independent variables or interactions to significantly affect the octahedral stresses at the 5% level of significance. Lug height did not significantly affect either σ_{oct} ($p = 0.6898$) or τ_{oct} ($p = 0.2173$), profile did not affect either σ_{oct} ($p = 0.9811$) or τ_{oct} ($p = 0.7728$), and depth did not affect either σ_{oct} ($p = 0.5982$) or τ_{oct} ($p = 0.7569$).

Comparison of the missing value analysis with the original data analysis shows that only a small percentage of SST pressure sensor pressures need be considerably higher than the mean pressures to cause a large reduction in the number of independent variables that significantly affect the dependent variables. The lack of significant effects of lug height on σ_{oct} and τ_{oct} in the original analysis indicates that the alignment of a lug end directly above an SST does not significantly affect the soil stresses when stress measurements are made at initial depths from 164 to 288 mm beneath the initial soil surface.

Soil Bulk Density

The dependent variable for the two analyses of variance, one for each soil, was the increase in dry bulk density of the three soil samples taken beneath the tire tracks in each plot, relative to loose soil. Dry bulk density was determined by extracting a cylindrical soil sample 69 mm in diameter and 40 mm in height, and dividing the mass of the oven-dried soil by the cylinder volume. Depths of the centers of soil samples taken from beneath the tire tracks, relative to the untrafficked soil surface, ranged from 202 to 355 mm in the NSL and 205 to 341 mm in the DCL. In each soil type, 72 bulk density measurements were made beneath the tire tracks. The coefficients of variation for the bulk density data were 5.8% in the NSL and 7.6% in the DCL. The lug height significantly affected the bulk density increase in both the NSL ($p = 0.0017$) and the DCL ($p = 0.0346$). The interaction of the soil profile and lug height significantly affected the bulk density increase in both soils ($p = 0.0001$), so lug height means were compared separately for each soil profile. In the uniform profile of the NSL and the hardpan profile of the DCL, some of the data exhibited an expected trend. The 100% lug height tire caused the greatest increase in bulk density and, in each case, the bulk density increase of the 100% tire was significantly greater than that of the 55% tire (table 8). Results from the hardpan profile of the NSL showed that the bulk density increase caused by the 55% lug height tire was significantly greater than that of the 31 or 100% tires. This result contradicted our expectation that bulk density increase would increase as lug height increased. In the uniform profile of the DCL, differences among the lug height means were not significant at the 5% level.

The soil profile significantly affected the bulk density increase in the NSL ($p = 0.0001$), but not in the DCL ($p = 0.1321$). In the NSL, the mean bulk density increase in the hardpan profile, 39.4%, exceeded that of the uniform profile, 32.2%. This difference exhibited the expected result that increases in bulk density are greater in soil above a hardpan than in a uniform profile.

In the NSL, the depth of the soil sample significantly affected the bulk density increase ($p = 0.0242$). The bulk density increase in the NSL exhibited an expected characteristic, that is, the bulk density increase decreased as depth increased (table 9). In the DCL, the interaction of depth and profile significantly affected the bulk density increase ($p = 0.0002$), so the effect of depth on bulk density increase was analyzed separately for each profile. In the DCL with the hardpan profile, the bulk density increase exhibited the same expected trend of decreasing bulk density increase with increasing depth that resulted for the NSL (table 9). In the uniform profile of the DCL, the bulk

Table 7. Effect of soil profile on σ_{oct} and τ_{oct} in the NSL soil for the missing value analysis

Profile	σ_{oct} (kPa)	τ_{oct} (kPa)
Uniform	76a*	86a
Hardpan	109b	128b

* Within columns, means followed by the same letter are not significantly different (alpha = 0.0001).

Table 3. Means of peak values of σ_{oct} and mean corresponding τ_{oct} for all treatments

		NSL						DCL					
		Deep Depth		Intermediate Depth		Shallow Depth		Deep Depth		Intermediate Depth		Shallow Depth	
Lug Height	Profile	σ_{oct} (kPa)	τ_{oct} (kPa)	σ_{oct} (kPa)	τ_{oct} (kPa)	σ_{oct} (kPa)	τ_{oct} (kPa)	σ_{oct} (kPa)	τ_{oct} (kPa)	σ_{oct} (kPa)	τ_{oct} (kPa)	σ_{oct} (kPa)	τ_{oct} (kPa)
31%	Uniform	75	82	77	80	64	72	79	116	111	195	102	143
55%	Uniform	69	73	81	84	76	110	99	151	120	213	81	104
100%	Uniform	80	105	80	84	78	84	81	111	93	140	82	113
31%	Hardpan	140	242	101	111	126	147	66	113	95	159	85	163
55%	Hardpan	109	134	100	107	104	103	68	79	101	121	73	88
100%	Hardpan	113	157	120	131	117	210	93	164	92	143	99	139

Table 6. Effect of lug height on σ_{oct} in the NSL soil for the missing value analysis

Lug Height	σ_{oct} (kPa)
100%	97.4a*
55%	89.9ab
31%	88.1b

* Means followed by the same letter are not significantly different at alpha = 0.05 (Duncan's multiple range test).

Table 8. Mean increases in soil bulk density as functions of lug height

	NSL		DCL	
Lug Height	Uniform Profile (%)	Hardpan Profile (%)	Uniform Profile (%)	Hardpan Profile (%)
100%	34.4a	35.4b	22.1a	24.3a
55%	30.0b	44.3a	22.2a	21.5b
31%	32.1ab	38.4b	24.1a	20.7b

Within columns, means followed by the same letter are not significantly different at alpha = 0.05 (Duncan's multiple range test).

Table 9. Mean increases in soil bulk density as functions of soil sample depth

Depth Designation	NSL (%)	DCL Uniform Profile (%)	DCL Hardpan Profile (%)
Shallow	36.7a	23.9a	25.5a
Intermediate	35.6ab	22.6a	22.4b
Deep	35.0b	21.9a	18.6c

Within columns, means followed by the same letter are not significantly different at alpha = 0.05 (Duncan's multiple range test).

density increase showed the same trend, but differences were not significant at the 5% level.

Bulk density is generally expected to increase as peak stresses in soil increase, but this was not always observed in this experiment. The tendency for the independent variables to have a significant effect on bulk density but not on soil stresses probably resulted from the greater variability of the stress data, relative to the bulk density data. This difference in variability is depicted by the greater coefficients of variation for stresses than for bulk density.

SUMMARY

Lug height did not significantly affect the peak octahedral normal stress and the corresponding octahedral shear stress in both the hardpan and uniform profiles of both the Norfolk sandy loam and Decatur clay loam soils. In the uniform profile of the sandy loam and in the hardpan profile of the clay loam, however, the new tire generated the greatest bulk density increases, which were significantly greater than those caused by the tire with 55% of the lug height of the new tire. In the sandy loam with the hardpan profile, the 55% tire generated a significantly greater bulk density increase than either the new or the 31% lug height tire.

In the sandy loam, both of the octahedral stresses were significantly greater in the hardpan profile than in the uniform profile. The bulk density increase in the hardpan profile of the sandy loam was significantly greater than that in the uniform profile.

The initial depth of the stress state transducers did not significantly affect the octahedral stresses when the depths ranged from 164 to 252 mm in the sandy loam and 164 to 288 mm in the clay loam soil. In the sandy loam and in the hardpan profile of the clay loam, the depth of soil samples significantly affected the bulk density increase for final depths relative to the untrafficked soil surface ranging from 202 to 335 mm in the sandy loam and from 205 to 341 mm in the clay loam. The increase in bulk density decreased monotonically as depth increased.

ACKNOWLEDGMENT. The authors acknowledge the contributions of Pirelli Armstrong Tire Corporation.

REFERENCES

ASAE Standards, 40th Ed. 1993. S296.3. Uniform terminology for traction of agricultural tractors, self-propelled implements, and other traction and transport devices. St. Joseph, Mich.: ASAE.

Bailey, A.C., T. A. Nichols and C. E. Johnson. 1988. Soil stress state determination under wheel loads. *Transactions of the ASAE* 31(5):1309-1314.

Burt, E. C., C. A. Reaves, A. C. Bailey and W. D. Pickering. 1980. A machine for testing tractor tires in soil bins. *Transactions of the ASAE* 23(3):546-547, 552.

Gee-Clough, D., M. McAllister and D. W. Evernden. 1977. Tractive performance of tractor drive tyres. I. The effect of lug height. *J. Agric. Eng. Res.* 22(4):373-384.

Grisso, R. D., C. E. Johnson and A. C. Bailey. 1987. Soil compaction by continuous deviatoric stress. *Transactions of the ASAE* 30(5):1293-1301.

Murphy, G. 1950. *Similitude in Engineering*, 12-13. New York: The Ronald Press Co.

Nichols, T. A., A. C. Bailey, C. E. Johnson and R. D. Grisso. 1987. A stress state transducer for soil. *Transactions of the ASAE* 30(5):1237-1241.

O'Brien, J. P. 1991. Worn drive tire traction performance. ASAE Paper No. 91-1586. St. Joseph, Mich.: ASAE.

Reed, I. F. and J. W. Shields. 1950. The effect of lug height and of rim width on the performance of farm tractor tires. SAE Nat. Tractor Meeting Paper No. 504. Warrendale, Pa.: SAE.

Vomocil, J. A., E. R. Fountaine and R. J. Reginato. 1958. The influence of speed and drawbar load on the compacting effect of wheeled tractors. *Soil Sci. Soc. Am. Proc.* 22(2):178-180.

MATHEMATICAL MODELING AND COMPUTER-AIDED DESIGN OF PASSIVE TILLAGE TOOLS

V. Ros, R. J. Smith, S. J. Marley, D. C. Erbach

ABSTRACT. *A method of designing tillage tool shapes based on mathematical expressions is needed. A mathematical equation for the macroshape of passive tillage tools is developed. The equation includes the main geometrical parameters and can be used for designing many different tillage tools. The mathematical description of tool geometry may determine how the design parameters influence the energy requirement and quality of operation. This description has the potential of achieving a quantitative analysis of the tillage process. A computer program has been developed to design and display selected passive tool shapes. The tool surface is represented by a multiplicity of quadrilateral faces limited by user-selected bounding curves. The (x,y,z) face coordinates are generated by a FORTRAN program and read into AutoCAD using an AutoLISP program. The method permits a complete study of the influence of the geometrical parameters upon the final soil condition and energy requirements, thus optimization of the tillage process may be possible.*

Keywords. *Tillage tools, Mathematical equation, Macrogeometry, Design, Computer-aided design.*

Tillage tools direct energy to the soil to cause some desired effect such as cutting, breaking, inversion, or movement of the soil, commonly at one pass. Soil is transformed from an initial condition (S_i) to a different final condition (S_f) by this process. The goal of tool design is to optimize the function, efficiency, and economy of the tillage process.

Agricultural implement design is hindered by a lack of adequate analytical methods, thus many implements are designed empirically (Gill and Vanden Berg, 1967; Schafer et al., 1985; Gebresenbet, 1991). True engineering design cannot be achieved until analytical relationships, based on scientific principles, are available.

In the past, much attention has been directed to tillage tool shape as related to energy requirements and final soil conditions. These investigations were concerned not only with macroshape but also with the boundary or edge of the tool (e.g., cutting edge). Also, because the area of the edges of a tool is generally much smaller than the area of the surface itself, much emphasis was placed on the surface over which the soil moves.

The moldboard plow is probably the classical answer to weed control (Kuipers, 1985); therefore, descriptions of the complex macrosurface of this tool have received much emphasis. One of the first methods for accurately describing the surface of a moldboard plow was developed by Thomas Jefferson (1799). It was a method based purely on intuition, but could be used to construct a practical plow bottom shape.

Quantitative descriptions of moldboard plow shapes have been developed by various researchers in attempts to correlate shape with function (e.g., White, 1918). Such correlations were seldom more than qualitative. Attempts were also made to relate shape to newly created soil conditions. Ashby (1931) defined a "slope coefficient" as a parameter of the shape of a plow bottom from a graphical representation of an existing shape. Soehne (1959) defined a number of parameters of shape description (the angles of the moldboard) and attempted to relate them to plow performance. He has demonstrated that more than one parameter of shape description can be obtained.

Goryachkin (1968) applied mathematics, physics, and engineering principles to the study of tillage tools and also related tool geometry to soil dynamics. His research clearly showed the potential role of soil dynamics in the design and use of soil-engaging machines. By 1920 he had developed a graphical theory of plow shape. Starting from Goryachkin's theory, many researchers developed graphical methods for the design and construction of tillage tools (Luchynskii, 1954; Barrett, 1967).

Nichols and Kummer (1932) stress that constant acceleration of the soil upon the surface is an important consideration in tillage tool design because this situation means that a constant pressure is being applied to the soil by the tool. Such is a necessary condition for uniform scouring and wear. The mechanical requirements of pulverization, turning, and inversion by uniform pressure surfaces whose sections have the indicated formulae (given by Nichols and Kummer) are suggested as bases for designing a tillage tool.

On the basis of Nichols and Kummer's theory, Carlson (1961) used the computer to analyze moldboard surfaces and soil movements over these surfaces. Richey et al. (1989) used a three-dimensional (3-D) bicubic surface

Article has been reviewed and approved for publication by the Power and Machinery Div. of ASAE. Presented as ASAE Paper No. 93-1091.

Joint contribution from the Agricultural Engineering Dept., Iowa State University, and Journal Paper No. J-15498 of the Iowa Agriculture and Home Economics Experiment Station , Ames, Project No. 2737, and from the USDA-Agricultural Research Service, National Soil Tilth Laboratory, Ames, Iowa. Trade and Company names are used solely to provide specific information and do not constitute a guarantee or an endorsement over other products not mentioned.

The authors are **Victor Ros**, Professor, Technical University of Cluj-Napoca, Romania; **Richard J. Smith**, Professor, **Stephen J. Marley**, ***ASAE Member Engineer***, Professor, Agricultural and Biosystems Engineering Dept., Iowa State University, Ames; and **Donald C. Erbach**, ***ASAE Member Engineer***, Agricultural Engineer, USDA-Agricultural Research Service, National Soil Tilth Laboratory, Ames, Iowa.